Journal of Hazardous Materials B114 (2004) 225–230

Journal of Hazardous Materials

www.elsevier.com/locate/jhazmat

Adsorption effect of aqueous bichlorobiphenyls onto UV-illuminated titanium dioxide

Chao-Yin Kuo*, Han-Yu Lin

Graduate Institute of Environmental and Safety Engineering, National Yunlin University of Science and Technology, Touliu, Yunlin 640, Taiwan

Received 13 April 2004; received in revised form 19 August 2004; accepted 20 August 2004
Available online 29 September 2004

Abstract

Bichlorobiphenyls were adsorbed onto TiO_2 (Degussa P25) in batch equilibrium experiments. The results demonstrated that a triple-layer model (TLM) surface complex formation model described the adsorption of chlorobiphenyls onto the surface of the TiO_2 solid. The surface complex configuration and the adsorption reaction may have followed the equation derived from the TLM, involving the loss of a proton during the adsorption process. This dependence indicates that the oxidation reaction between surface-adsorbed substrates and photogenerated oxidants dominates. Both sorbed and dissolved components contribute to the observed degradation rate, that is, the 4,4′-CBP degradation rates might be stated as linear functions of the sorbed and dissolved concentrations. The contribution of the concentration of solution phase in degradation pathways is not negligible.

Keywords: Bichlorobiphenyls; Adsorption; Titanium dioxide; Triple-layer model

1. Introduction

Although the production of polychlorinated biphenyls (PCBs) was banned in 1977, PCBs released into the environment remain some of the most widespread pollutants in the global ecosystem [1–3]. PCBs are of environmental concern because their presence is widespread; they are persistent; they accumulate in biota, and they have carcinogenic effects on humans [4]. PCBs are somewhat resistant to the usual mechanisms of environmental degradation. They are globally distributed and characterized by half-lives of many months in the atmosphere, but 3–7 years in lakes [5].

In most natural waters, PCBs are found in the aqueous phase and associated with particulate matter [6]. The fraction of PCB in each phase is a function of the hydrophobicity of the congener. Congeners that contain more chlorine are more likely to be associated with particulates.

4-Chlorobiphenyl (4-CBP) and 4,4′-bichlorobiphenyl (4,4′-CBP) are PCBs with of low solubility and a tendency to be adsorbed onto solid surfaces [3,7]. The solution and interfacial adsorption of nonionic surfactants on hydrophobic surfaces are very important. The presence of particulates may encourage or reduce the oxidation of 4-CBP or 4,4′-CBP, and the kinetics of sorption must be understood before the rates of transformation can be predicted; however, little information is available regarding the adsorption of chlorobiphenyl onto TiO_2. Because adsorption is defined at the solid/liquid interface of a system at electrochemical equilibrium, the triple-layer model (TLM) is employed to relate charge densities to interfacial potential profiles and the 4-CBP and 4,4′-CBP adsorption might use a TLM to simulate. These studies address photocatalytic oxidation (PCO) of organic compounds [8–12] in the presence of suspended TiO_2 particles and irradiation under simulated solar light. When exposed to light with wavelengths under 380 nm, conduction band electrons, including electron vacancies, and valence band holes, are generated on the surface of titanium dioxide particles [13–15]. Hence, the significance of the adsorption reaction between chloro-

* Corresponding author. Fax: +886 5 5312069.
E-mail addresses: kuocyr@ms35.hinet.net, kuocy@yuntech.edu.tw (C.-Y. Kuo).

0304-3894/$ – see front matter © 2004 Elsevier B.V. All rights reserved.
doi:10.1016/j.jhazmat.2004.08.018

biphenyls and TiO_2 cannot be ignored. The hole scavenges an electron from a hydroxylated TiO_2 surface species, generating an OH radical. The OH radical is a powerful nonselective oxidants. Reactions of OH radicals with organic compounds yield various organic intermediates, which may eventually be mineralized to CO_2.

2. Materials and methods

2.1. Analytical methods

The specific surface area of TiO_2 (Degussa, P25, primarily anatase, nonporous) was 53 m^2/g, as determined by the BET-N_2 method, using a Model ASAP-2000 from Micrometrics Instrument Corporation. TiO_2 P25 was carefully washed in water and irradiated in a solar box for a few hours, to decompose any organic impurities present in the starting material. The treated semiconductor was then dried in an oven at 80+. Purification of TiO_2 P25 was performed by modifying procedures for purifying γ-Al_2O_3 [16].

4-Chlorobiphenyl (4-CBP) and 4,4′-bichlorobiphenyl (4,4′-CBP) (Chem Service Co., S.G. grade 99+%) were selected as model compounds. Methanol 1% as a dispersion medium (Merck, G.R. grade), containing 4-CBP and 4,4′-CBP, was used as the stock solution (50 mg/L), which was diluted with deionized water (Milli-Q SP) to the required concentration before use. All other agents used were purchased from Merck, and were G.R. grade. 4-CBP, 4,4′-CBP and intermediates were analyzed by GC/ECD or GC/MS. All detailed analyses strictly followed the QA/QC method to ensure the accuracy of the results.

2.2. Adsorption experiment

Experiments were conducted to elucidate the adsorption of aqueous 4-CBP and 4,4′-CBP onto glass and TiO_2. The initial pH of a series of amber glass bottles, each containing 100 mL of chlorobiphenyl at various concentrations, was adjusted to values between 2 and 11, by adding 1 M NaOH and/or HNO_3. A specific quantity of TiO_2 was then added. Background concentrations of electrolyte $NaNO_3$ were added to the bottles to maintain ionic strength, and adjusted to 0.01 M. The samples were placed on a shaker and mixed at 150 rpm.

After equilibration, the pH of each suspension was ascertained. Each suspension was centrifuged at 9500 rpm for 10 min, and the supernatant was then filtered through 0.2 μm filter paper (Gelman Sciences). Analysis followed the microextraction of chlorobiphenyls from 10 mL of the supernatant using 5 mL of *n*-hexane. The mixture was mechanically shaken for 20 min and the microextraction liquor was then analyzed on GC.

2.3. Adsorption model

The triple-layer model (TLM) is employed to relate charge densities to interfacial potential profiles. The experimentally

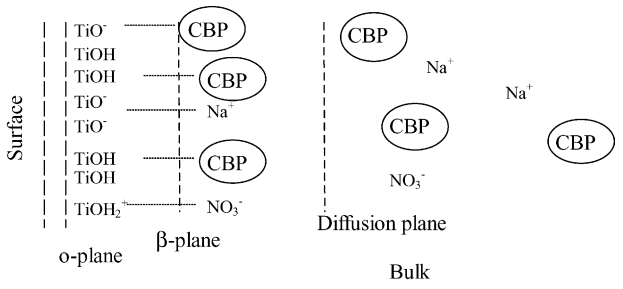

Fig. 1. Schematic representation of the interface of TiO_2 in the presence of adsorbed chlorobiphenyls.

observed 4-CBP and 4,4′-CBP adsorption are represented using a TLM, as proposed by Davis and Leckie [17], and subsequently modified by Hayes and Leckie [18]. The modified TLM differs from the original model in two ways. First, the adsorbed ion can be located on both the o-layer and the β-layer; that is ions may form either inner-(o-layer) or outer-(β-layer) sphere surface complexes. Second, the chemical potential and standard and reference states are defined equivalently for both solution and surface species, leading to a relationship between the activity coefficients and the interfacial potential that is different from that previously established.

Adsorption is defined at the solid/liquid interface of a system at electrochemical equilibrium. The adsorptions of 4-CBP and 4,4′-CBP were assumed to be proportional to the number of bonds between their functional groups and those of the surface. 4-CBP and 4,4′-CBP were adsorbed onto the surface of TiO_2, are shown in Fig. 1.

The surface hydroxyl groups (TiOH) can take up and release protons to form positive ($TiOH_2^+$) and negative (TiO^-) sites. These charged sites can also adsorb ions from the solution, forming complex species such as ($TiOH_2^+ + NO_3^-$) or ($TiO^- + Na^+$). All calculations were based on according to the modified TLM model.

2.4. Photocatalytic oxidation

The experimental arrangement used for the study of photocatalysis has been described elsewhere [8], and involves five main parts: (1) a 500 W blacklight UV fluorescent tube (Oriel 6285, mercury lamp); (2) $HClO_4$ and/or NaOH, used as sources to control the pH (Toho Kagaku, PET 300 A); (3) a double-layer glass batch reactor (Iwaki Code 7740) with an external diameter of 12 cm, an internal diameter of 10 cm and a height of 23 cm; (4) a double-layer quartz tube used as a substitute for the UV tube, between both of which layers, cooling water was recycled between these two glass layers; (5) a stirrer (FG Fargo MS 203) placed at the bottom of the photoreactor to mix the solution.

Photocatalytic oxidation experiments were undertaken to elucidate the correlation between the concentration of chlorobiphenyls sorbed onto TiO_2 and the concentration of dissolved chlorobiphenyls. Five hundred micrograms per liter of chlorobiphenyl was placed in a photoreactor, and TiO_2 was

added to various concentrations in each experiment; 30 min later, chlorobiphenyls had been adsorbed onto TiO_2 and the UV light was turned on. Following various periods of photocatalytic oxidation, all of the solution was removed to extract and analyze its concentration in the solution phase as C_s; chlorobiphenyls were desorbed from TiO_2 using 10 mL of 12 M NaOH for ten hours and chlorobiphenyls sorbed onto reaction wall were ignored because the amounts of adsorption onto reaction wall were less than 5% as previous work [8] during reaction time to 180 min. Then, the supernatant was all removed to analyze the concentration which had adsorbed as C_a. After various periods of photocatalytic oxidation and following desorption, the suspensions were pretreated, prepared and analyzed as in the adsorption experiments.

This investigation addresses parameters, including surface loading and pH, that may affect the adsorption of 4-CBP and 4,4′-CBP onto TiO_2 (anatase) particles. The adsorption of 4-CBP and 4,4′-CBP at the TiO_2 (anatase)/solution interface was elucidated, and the results were used to derive the correlation between the concentration of 4-CBP or 4,4′-CBP sorbed onto TiO_2 and that of 4-CBP or 4,4′-CBP in solution, during photocatalytic oxidation.

3. Results and discussion

3.1. Simulation results concerning adsorption of TLM onto hydrous TiO_2

Surface acidity is an important characteristic of hydrous solids, and is related to the extent of interfacial reactions, such as the adsorption of metals [19]. Table 1 lists the intrinsic reaction constants and other parameters associated with TLM. Potentiometric titration experiments on 0.1 g/L titanium dioxide suspensions with three different background electrolyte concentrations (0.1, 0.01, and 0.001N) were conducted to determine K^{int}_{a1}, K^{int}_{a2}, $K^{int}_{Na^+}$ and $K^{int}_{NO_3^-}$, as described by Davis and Leckie [17]. The acidity constants were obtained by extrapolating the titration data at the lowest $NaNO_3$ concentration to zero fractional ionization. The $\log K^{int}_{a1}$, $\log K^{int}_{a2}$, $\log K^{int}_{Na^+}$ and $\log K^{int}_{NO_3^-}$ values were −5.0, −8.0, −8.5, and 7.5, respectively. For comparison, the $\log K^{int}_{a1}$ and $\log K^{int}_{a2}$ values reported by Hohl and Stumm [16] were −7.2 and −9.5. The $\log K^{int}_{Na^+}$ and $\log K^{int}_{NO_3^-}$ values reported by Zhang and Sparks [20] and Hayes and Leckie [18] were −9.1 and 8.7. The reactions and equilibrium expressions assumed in the TLM are summarized below:

$$TiOH_2^+ = TiOH + H^+ \quad (1)$$

$$TiOH = TiO^- + H^+ \quad (2)$$

$$TiOH + Na^+ = TiO^- - Na^+ + H^+ \quad (3)$$

$$TiOH + H^+ + NO_3^- = TiOH_2^+ - NO_3^- \quad (4)$$

$$TiOH + PCB = TiOH - PCB \quad (5)$$

$$TiOH + PCB = TiO^- - PCB + H^+ \quad (6)$$

The intrinsic conditional equilibrium constants of these reactions are defined as

$$K^{int}_{a1} = \frac{\{TiOH\}\{H^+\}}{\{TiOH_2^+\}} \exp\left(\frac{-\psi_o F}{RT}\right) \quad (7)$$

$$K^{int}_{a2} = \frac{\{TiO^-\}\{H^+\}}{\{TiOH\}} \exp\left(\frac{-\psi_o F}{RT}\right) \quad (8)$$

$$K^{int}_{Na^+} = \frac{\{TiO^- - Na^+\}\{H^+\}}{\{TiOH\}\{Na^+\}} \exp\left[\frac{(\psi_\beta - \psi_o)F}{RT}\right] \quad (9)$$

$$K^{int}_{NO_3^-} = \frac{\{TiOH_2^+ - NO_3^-\}}{\{TiOH\}\{H^+\}\{NO_3^-\}} \exp\left[\frac{(\psi_0 - \psi_\beta)F}{RT}\right] \quad (10)$$

$$K^{int}_{PCB} = \frac{\{TiOH - PCB\}}{\{TiOH\}\{PCB\}} \quad (11)$$

$$K^{int}_{PCB} = \frac{\{TiO^- - PCB\}\{H^+\}}{\{TiOH\}\{PCB\}} \exp\left(\frac{-\psi_o F}{RT}\right) \quad (12)$$

where R is the gas constant; T the absolute temperature; F the Faraday constant; ψ_o the surface potential on the o-plane, and ψ_β the surface potential on the β-plane (see Fig. 1).

Eqs. (1), (2), (7) and (8) describe the protonation of reacting surface sites, and Eqs. (3), (4), (9) and (10) describe the formation of complexes between the background electrolyte ions and the surface. A set of possible reactions (Eqs. (5), (6), (11) and (12)) between chlorobiphenyls and the functional groups on the surface of the TiO_2 solids can be expressed with reference to the TLM model.

4-CBP or 4,4′-CBP are generated on the β-plane (Eqs. (5) and (6)), where the adsorption is nonspecific and the reaction product is an outer-sphere surface complex. Eq. (5) presents 4-CBP or 4,4′-CBP generated on the β-plane of TiO_2 without releasing hydrogen ion, but Eq. (6) does. The other adsorption reactions can, however, be expressed as an inner-sphere surface coordination process if the adsorption of 4-CBP or 4,4-CBP were considered to be a chemically specific reaction, but the results of simulation we did were all unsuitable and did not show in this paper.

Fig. 2 depicts the sorption envelopes of 500 μg/L 4,4′-CBP on 0.1 g/L TiO_2 in the presence of 0.01N $NaNO_3$ electrolyte. Kuo and Lo [8] reported 4-CBP on 0.1 g/L TiO_2 in the presence of 0.01N $NaNO_3$. The sorption density of 4,4′-CBP increases as the system shifts from acidic to alkaline.

Table 1
Numerical values of the adsorption parameters used in the TLM calculation

Specific surface area (m^2/g)	53
Site density (sites/nm^2)	5
C_1 (o-plane capacitance, μF/cm^2)	80 [25]
C_2 (β-plane capacitance, μF/cm^2)	20 [25]
$\log K^{int}_{a1}$, $\log K^{int}_{a2}$	−5.0, −8.0
$\log K^{int}_{Na^+}$, $\log K^{int}_{NO_3^-}$	−9.1, 8.7 [18,20]

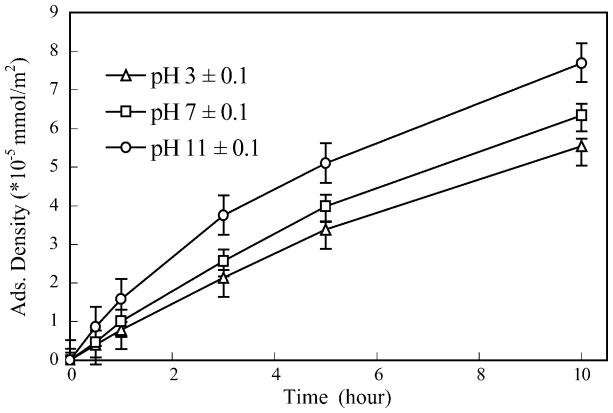

Fig. 2. Variation of 4,4′-CBP adsorption density (Γ) on TiO_2 with time at different pH (4,4′-CBP initial conc. = 500 μg/L, 20 °C).

At higher pH, more sites are negatively charged, increasing the attraction between the surface of TiO_2 and the PCB, thereby increasing the extent of adsorption. In Fig. 3, Eqs. (5) and (6) can almost be applied to nonelectric complexes (TiOH–4-CBP) and electric complexes (TiO^-–4-CBP), but at lower pH, more sites are nonelectric, increasing the attraction between the surface of TiOH and the 4-CBP, and at higher pH, more sites are negatively charged, increasing the attraction between the surface of TiO^- and the 4-CBP, thereby increasing the fitting of adsorption Eq. (5). In addition, in Fig. 3, Eq. (5) cannot be applied to nonelectric complexes (TiOH–4,4′-CBP), however, Eq. (6) can be fitted. Since high pH causes more sites of TiO_2 surface to become negatively charged like as TiO^-, and causes 4,4-CBP one more chlorine atom to become partially positively charge, adsorption of 4,4-CBP increases at the surface of TiO^-, thereby increasing the fitting of adsorption Eq. (6). The fitted intrinsic formation constants of TiO^-–4-CBP and TiO^-–4.4′-CBP were $10^{2.4}$ and $10^{2.1}$, respectively. Eq. (6) yields the surface complex configuration of the surface and the adsorption reaction.

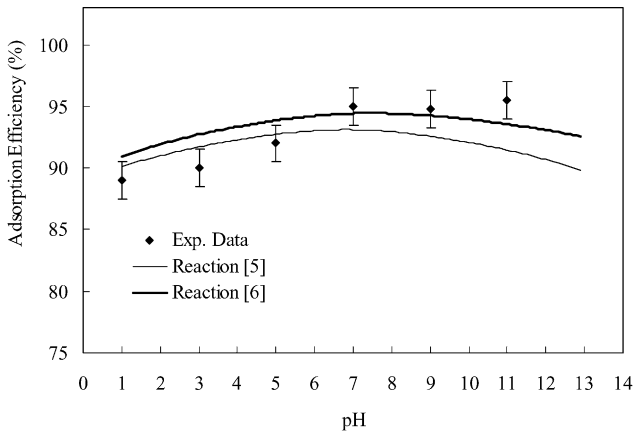

Fig. 3. Simulation of TLM for 4-CBP adsorption on TiO_2 at 0.1 g/L (4-CBP initial conc.= 500 μg/L, 24 h, 20 °C).

Table 2
Simulation of Langmuir first-order reaction for 4,4′-CBP adsorbed onto TiO_2 (20+)

	k (M/s)	pK	R^2
pH 3 ± 0.1	7.4×10^{-10}	4.58	0.98
pH 7 ± 0.1	6.7×10^{-10}	4.73	0.96
pH 11 ± 0.1	7.4×10^{-10}	4.87	0.92

3.2. Rate of adsorption and equilibrium adsorption

The relationship between the reaction rate and the surface coverage of the reaction is assumed to be a first-order reaction, known as a Langmuir first-order reaction. Table 2 states the values of k (adsorption rate constant), of around 7.4×10^{-10} M/s for 4,4′-CBP; $-\log K$ (adsorption equilibrium constant), of approximately 4.73 for 4,4′-CBP, and R squared (>0.92 for 4,4′-CBP) for this reaction. 4-CBP data have been provided elsewhere [8]. The results imply that k and K were almost constant under experimental conditions except at high pH, such that k and K simulated for the Langmuir first-order reaction were almost independent of pH. The greater adsorption of 4,4′-CBP, however, occurred at higher pH.

3.3. UV/TiO_2 process

The degradation rates for photocatalysis on TiO_2 normally are consistent with Langmuir–Hinshelwood kinetics [10,21–23]. This dependence is such that the reaction between surface-adsorbed substrates and photogenerated oxidants dominates. However, numerous studies of both sorption and photoreactivity on TiO_2 seem to indicate that the reaction mechanisms are more complex than indicated by a simple Langmuir–Hinshelwood analysis.

Tunesi and Anderson [24] studied the adsorption and photoreactivity of a range of substituted benzenes, including phenol and salicylate. The first-order degradation rate of salicylate was also higher at lower pH, implying that the sorbed concentration was positively correlated with the observed rate of degradation. However, at low pH, as the concentration of the salicylate solution was increased, the first-order degradation rate declined (Fig. 4).

Experimental results demonstrated (Figs. 5 and 6) that the initial concentration of adsorbed 4,4′-CBP plus that of dissolved 4,4′-CBP was approximately 500 μg/L, at the initial concentration, and almost reached mass balance. The experimentally observed degradation rates at all pH values were more closely correlated to the sorbed 4,4′-CBP concentration than to the corresponding concentration in the aqueous phase. However, given the quality of the fits in Figs. 5 and 6, the possibility that both sorbed and dissolved components contribute to the observed degradation rate cannot be eliminated.

The sorbed and dissolved components exhibit the modified first-order reaction,

$$r = -\frac{\mathrm{d}[C]}{\mathrm{d}t} = k_a C_a + k_s C_s \quad (13)$$

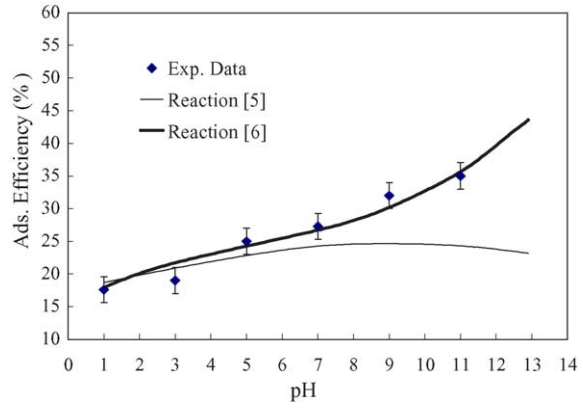

Fig. 4. Simulation of TLM for 4,4′-CBP adsorption on TiO_2 at 0.1 g/L (4,4′-CBP initial conc. = 500 μg/L, 24 h, 20 °C).

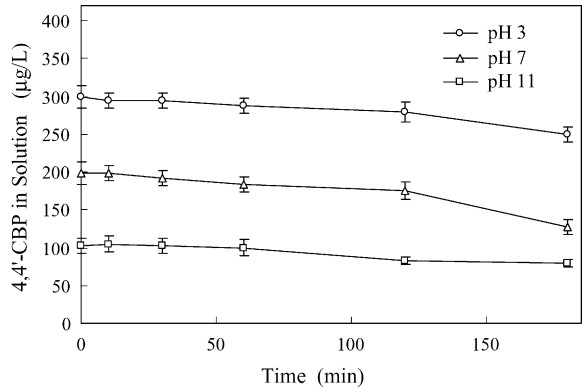

Fig. 5. Variation of 4,4′-CBP concentration in solution with time during the UV/TiO_2 process at different pH (4,4′-CBP initial conc. = 500 μg/L, TiO_2 = 1 g/L, methanol = 1%, 20 °C, UV light intensity = 10 mW/cm^2).

where k_a is the experimental rate constant of the pseudo-first-order reaction of the adsorbed phase with oxidants formed by the illuminating TiO_2; C_a represents the concentration of 4,4′-CBP in the adsorbed phase; k_s represents the pseudo-first-order reaction rate of the solution phase; C_s represents the concentration of dissolved 4,4′-CBP.

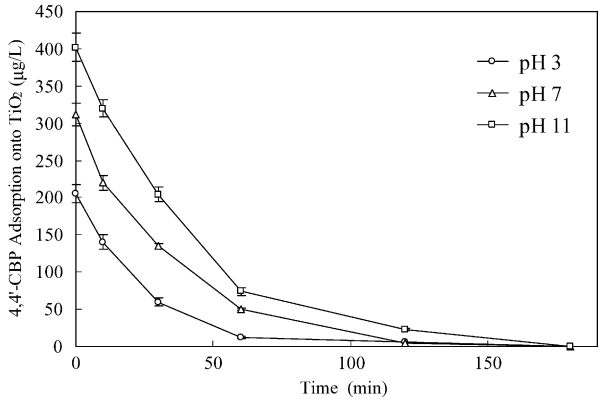

Fig. 6. Variation of 4,4′-CBP adsorption onto TiO_2 with time during the UV/TiO_2 process at different pH (the same conditions as Fig. 5).

Table 3
Simulation of modified first-order reaction for 4,4-CBP using the UV/TiO_2 process (20+) (TiO_2 = 1 g/L)

	pH 3	pH 7	pH 11
k_s (s^{-1})	9×10^{-6}	1×10^{-5}	1×10^{-5}
k_a (s^{-1})	2×10^{-4}	2×10^{-4}	2×10^{-4}
R^2	0.93	0.95	0.97

Table 3 presents k_s and k_a values at each pH value at 20+ in 1.0 g/L TiO_2. The results reveal that k_a is almost 10 times than k_s. Accordingly, the rates of degradation of 4,4′-CBP can be stated as linear functions of the sorbed and dissolved concentrations, with negligible contributions by the solution phase in degradation. The results may indicate that, at high pH, 4,4′-CBP is degraded by the direct oxidation of adsorbed 4,4′-CBP. At lower pH, when 4,4′-CBP is not strongly adsorbed, more degradation occurs in the solution.

Little attention has so far been paid to the generation of important dangerous intermediates during photocatalytic oxidation or noxious by-products. Therefore, identifying all possible intermediate compounds is important. Chlorohydroxy derivatives of biphenyls, chlorohydroquinone, catechol, dichlorocatechol and dichlororesorcinol were revealed in the photocatalytic oxidation process, using GC/MS. In the experiments conducted herein, the total degradation of the target compound did not always correspond to the complete mineralization of the organics to CO_2 and H_2O in the early reaction period even when the target compound was degraded.

4. Conclusion

This study proposes adsorption reactions between chlorobiphenyls and the functional groups at the surface of TiO_2 solids, which can be expressed with reference to the TLM model. The fitted intrinsic formation constants of TiO^-–4-CBP and TiO^-–4.4′-CBP are $10^{2.4}$ and $10^{2.1}$, respectively.

In this study, the experimentally determined rates of degradation at all pH values are more strongly correlated to the sorbed 4,4′-CBP concentration than to the corresponding aqueous concentration; however, the possibility that both sorbed and dissolved components contribute to the observed degradation rate cannot be eliminated. The results are consistent with a modified first-order reaction, so at high pH, 4,4′-CBP was degraded by the direct oxidation of adsorbed 4,4′-CBP and at lower pH, degradation was via solution.

Acknowledgements

The authors thank the reviewers for their constructive comments. The authors also express their sincere thanks to the National Science Council of the Republic of China for financially supporting this research under Contract No. NSC 92-2211-E-224-003 and NSC 93-2211-E-224-001.

References

[1] B. Tartakovsky, J. Hawari, S.R. Guiot, Enhance dechlorination of aroclor1242 in an anaerobic continuous bioreactor, Water Res. 34 (2000) 85–92.

[2] R.N. Dexter, S.P. Pavlou, Distribution of stable organic molecules in marine environment: physical–chemical aspects chlorinated hydrocarbons, Mar. Chem. 7 (1978) 67–78.

[3] S. Sun, W.P. Inskeep, Sorption of nonionic organic compounds in soil–water systems containing a micelle-forming surfactant, Environ. Sci. Technol. 29 (1995) 903–915.

[4] J.A. Bumpus, M. Tien, D. Wright, S.D. Aust, Oxidation of persistent environmental pollutants by a white rot fungus, Science 228 (1985) 1434–1436.

[5] G. Zhang, A.I. Hua, Cavitation chemistry of polychlorinated biphenyls: decomposition mechanisms and rates, Environ. Sci. Technol. 34 (2000) 1529–1534.

[6] D.L. Sedlak, A.W. Andren, The effect of sorption on the oxidation of polychlorinated biphenyls (PCBs) by hydroxyl radical, Water Res. 28 (1994) 1207–1218.

[7] D.J. Widish, C.D. Metcalfe, H.M. Akai, D.W. Mcleese, Flux of aroclor 1254 between sediment and water, Bull. Environ. Contam. Toxical. 24 (1980) 20–34.

[8] C.Y. Kuo, S.L. Lo, Adsorption of aqueous 4-chlorobiphenyl and treatment with UV-illuminated titanium dioxide, J. Colloid Interf. Sci. 196 (1997) 199–207.

[9] C.Y. Kuo, S.L. Lo, Oxidation of aqueous chlorobiphenyls with photo-fenton process, Chemosphere 38 (1999) 2041–2051.

[10] T.M. El-Morsi, W.R. Budakowski, A.S. Abd-El-Aziz, K.J. Friesne, Photocatalytic degradation of 1,10-dichlorodecane in aqueous suspensions of TiO_2: a reaction of adsorbed chlorinated alkane with surface hydroxyl radicals, Environ. Sci. Technol. 34 (2000) 1018–1022.

[11] A. Kumar, A.K. Jain, Photophysics and photochemistry of colloidal Cds-TiO_2 coupled semiconductors-photocatalytic oxidation of indole, J. Mol. Catal. A: Chem. 165 (2001) 265–273.

[12] B. Nepploian, H.C. Choi, S. Sakthivel, B. Arabindoo, V. Murugesan, Solar/UV-induced photocatalytic degradation of three commercial textile dyes, J. Hazard. Mater. B 89 (2002) 303–317.

[13] C.S. Turchi, D.F. Ollis, Photocatalytic degradation of organic water contaminats: mechanisms involving hydroxyl radical attack, J. Catal. 122 (1990) 178–192.

[14] M.S. Vohra, K. Tanaka, Photocatalytic degradation of aqueous pollutants using silica-modified TiO_2, Water Res. 37 (2003) 3992–3996.

[15] L. Li, W. Zhu, P. Zhang, Z. Chen, W. Han, Photocatalytic oxidation and ozonation of catechol over carbon-black-modified nano-TiO_2 thin films supported on Al sheet, Water Res. 37 (2003) 3646–3651.

[16] M. Hohl, W. Stumn, Interaction of Pb^{2+} with hydrous γ-Al_2O_3, J. Colloid Interf. Sci. 55 (1976) 281–294.

[17] J.A. Davis, J.O. Leckie, Surface ionization and complexation at the oxide/water interface. II. Surface properties of amorphous iron oxyhydroxide and adsorption of metal ions, J. Colloid Interf. Sci. 67 (1978) 90–98.

[18] K.F. Hayes, J.O. Leckie, Modeling ionic strength effects on cation adsorption at hydrous oxide/solution interfaces, J. Colloid Interf. Sci. 115 (1987) 564–572.

[19] C.H. Weng, J.H. Wang, C.P. Huang, Adsorption of Cr(+) onto TiO_2 from dilute aqueous solutions, Water Sci. Technol. 35 (1997) 55–62.

[20] P.C. Zhang, D.L. Sparks, Kinetics of selenate and selenite adsorption/desorption at the goethite/water Interface, Environ. Sci. Technol. 24 (1990) 1848–1856.

[21] C. Kormann, D.W. Bahnemann, M.R. Hoffmann, Photolysis of chloroform and other organic molecules in aqueous TiO_2 suspensions, Environ. Sci. Technol. 25 (1991) 494–500.

[22] A. Mills, S. Morris, Photomineralization of 4-chlorophenol sensitized by titanium dioxide: a study of the initial kinetics of carbon dioxide photogeneration, J. Photochem. Photobiol. A 71 (1993) 75–83.

[23] Y. Ku, I.L. Jung, Photocatalytic reduction of Cr(+) in aqueous solutions by UV-irradiation with the presence of titanium dioxide, Water Res. 35 (2001) 135–142.

[24] S. Tunesi, M. Anderson, Influence of chemisorption on the photodecomposition of salilcylic acid and related compounds using suspended TiO_2 ceramic membranes, J. Phys. Chem. 95 (1991) 3399–3405.

[25] K.F. Hayes, G. Redden, W. Ela, J.O. Leckie, Surface complexation models: an evaluation of model parameter estimation using FITEQL and oxide mineral titration data, J. Colloid Interf. Sci. 142 (1991) 448–461.